Electronic Supplementary Material (ESI) for Dalton Transactions.

Metal-Organic Frameworks Based on Rigid Ligands as Separator Membranes in Supercapacitor

Jiang-Ping Meng, [a] Yun Gong, *[a] Qiang Lin, [a] Miao-Miao Zhang, [a] Pan Zhang, [a] Hui-Fang Shi [a] and Jian-Hua Lin* [a,b]

[a] *College of Chemistry and Chemical Engineering, Chongqing University, Chongqing 400030, P. R. China Tel: +86-023-65106150 E-mail: gongyun7211@cqu.edu.cn*

[b] *Zhejiang University, Hangzhou 310058, P. R. China Tel: +86-0571-88981583 E-mail: jhlin@cqu.edu.cn; jhlin@zju.edu.cn; jhlin@pku.edu.cn*

Supporting Information

Synthesis of CoL(4,4'-bpc)·2DMF (**3**): The synthesis of MOF **2** was carried out as described above for complex **2** except that $Co(NO_3)_2·6H_2O$ was used instead of $Cd(NO_3)_2·4H_2O$. The yield of the red block crystals is ca. 70 % based on **L**. Elemental Anal. Found: C, 57.55; H, 4.50; N, 18.78 %. Calcd. for $CoC_{39}H_{35}N_{11}O_6$: C, 57.64; H, 4.34; N, 18.96 %. IR (cm^{-1}): 3397(s), 2922(w), 2359(w), 1657(s), 1616(s), 1586(s), 1531(s), 1402(s), 1384(s), 1103(w), 1018(w), 845(m), 801(m), 772(s), 698(m), 534(w), 432(w).

Crystal data for MOF **3**: $CoC_{39}H_{35}N_{11}O_6$, M = 812.71, monoclinic, a = 11.0020(6), b = 22.1547(17), c = 16.9957(9) Å, β=100.697(5) ℃, V = 4070.6(4) Å^3, T = 293(2) K, space group $P2_1/c$, Z = 4, μ= 1.207 mm^{-1}, 7130 reflections measured, 7130 unique which were used in all calculations. R_1 = 0.0567 and wR_2 = 0.1542 for $I > 2\sigma(I)$. CCDC: 1044074). The solvent molecule in MOF **3** was highly disordered and was impossible to refine using conventional discrete-atom models, thus the contribution of partial solvent electron densities were removed by the SQUEEZE routine in PLATON. The final chemical formula of MOF **3** was estimated from the SQUEEZE result combined with the TGA result.

Crystal Structure of CoL(4,4'-bpc)·2DMF (**3**) Single-crystal X-ray diffraction analyses reveal that the compositions of MOFs **2** and **3** are similar except for different metal(II) ions in the structures. The Co-N and Co-O distances are in the range of 2.150(3)- 2.155(3) and 2.008(2)- 2.264(2) Å, respectively (**Table S1**). The dihedral angle between the two phenyl rings of the crystallographically independent 4,4'-bpc^{2-} is 37.4 º. And the dihedral angles between the neighboring pyridine ring and triazol ring of the crystallographically independent **L** ligand is in the range of 4.6-9.9º. The solvent-accessible volume of the unit cell of MOF **3** is 1586.2 Å^3, which is approximately 39.0 % of the unit-cell volume (4070.7 Å^3).

Table S1 Selected bond lengths (Å) and angles (º) for MOFs **1**-**3**.

*MOF **1***			
Co(1)-N(1)	2.179(4)	Co(1)-O(4)#1	1.933(5)
Co(1)-O(3)#2	2.051(4)	Co(1)-O(2)	2.360(7)
O(1)-Co(1)-O(2)	59.1(2)	O(3)#2-Co(1)-O(1)	146.0(3)
O(4)#1-Co(1)-O(1)	85.9(3)	N(1)-Co(1)-N(1)#3	179.52(13)
O(3)#2-Co(1)-N(1)	89.77(6)	O(1)-Co(1)-N(1)	90.23(6)
*MOF **2***			
Cd(1)-N(1)	2.315(4)	Cd(1)-O(2)#4	2.182(4)
Cd(1)-O(3)#5	2.460(4)	Cd(1)-N(9)#6	2.326(4)
O(4)#5-Cd(1)-O(3)#5	55.05(13)	O(1)-Cd(1)-O(4)#5	145.03(16)

O(1)-Cd(1)-O(3)#5	90.11(15)	N(1)-Cd(1)-N(9)#6	170.44(17)
O(1)-Cd(1)-N(9)#6	84.25(17)	O(2)#4-Cd(1)-N(1)	101.76(17)
MOF 3			
Co(1)-N(1)	2.150(3)	Co(1)-N(9)#6	2.155(3)
Co(1)-O(2)	2.008(2)	Co(1)-O(4)#7	2.264(2)
O(3)#7-Co(1)-O(4)#7	59.32(8)	O(1)#1-Co(1)-O(3)#7	150.77(9)
O(2)-Co(1)-O(3)#7	90.93(9)	N(1)-Co(1)-N(9)#6	174.52(11)
O(1)#8-Co(1)-N(1)	86.42(10)	O(2)-Co(1)-N(9)#6	96.35(10)

Symmetry transformations used to generate equivalent atoms:

#1 -x+1/2, -y+1, z-1/2 #2 x+1/2, y, -z+3/2 #3 x, -y+1, z #4 -x+1,-y+1,-z+1
#5 -x,y-1/2,-z+1/2 #6 x-1,y,z+1 #7 x+1,-y+3/2,z+1/2 #8 -x,-y+1,-z+1

(a) (b)

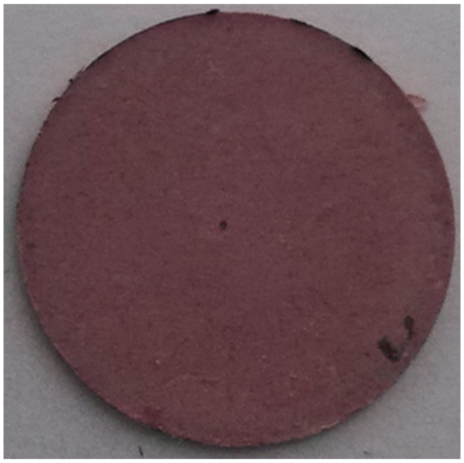

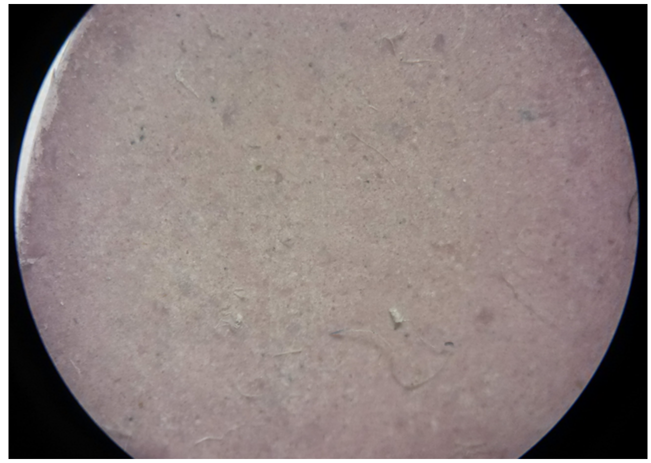

(c) (d)

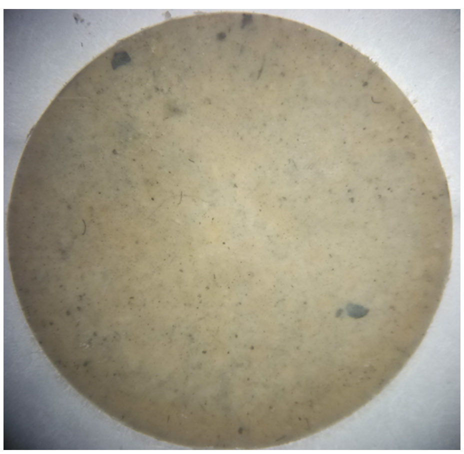

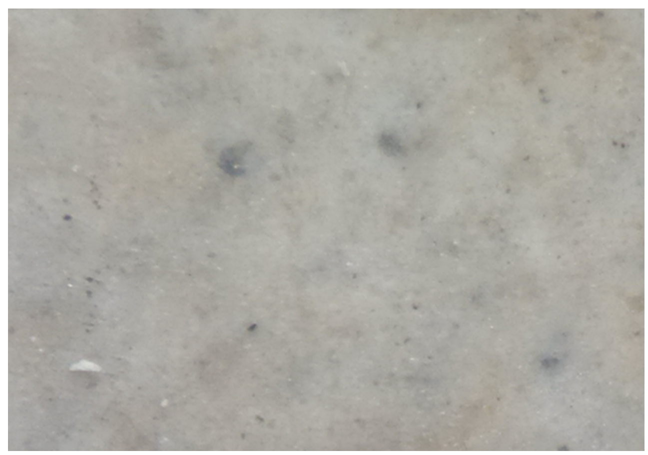

Fig. S1 The photographs and optic micrograms (40-fold magnified) of the separator membranes of MOFs **1** (**a, b**) and **2** (**c, d**).

(a) (b)

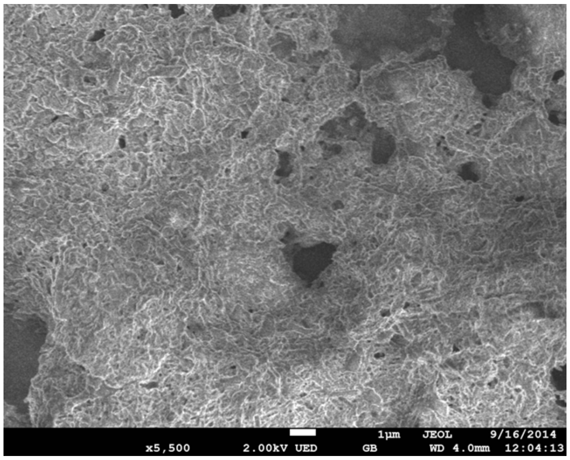
1μm JEOL 9/16/2014
x5,500 2.00kV UED GB WD 4.0mm 12:04:13

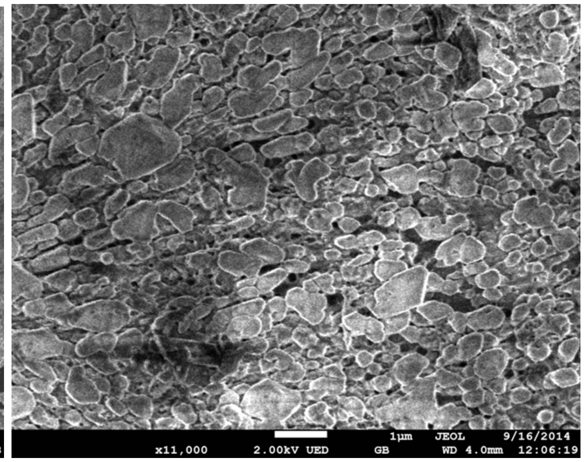
1μm JEOL 9/16/2014
x11,000 2.00kV UED GB WD 4.0mm 12:06:19

(c) (d)

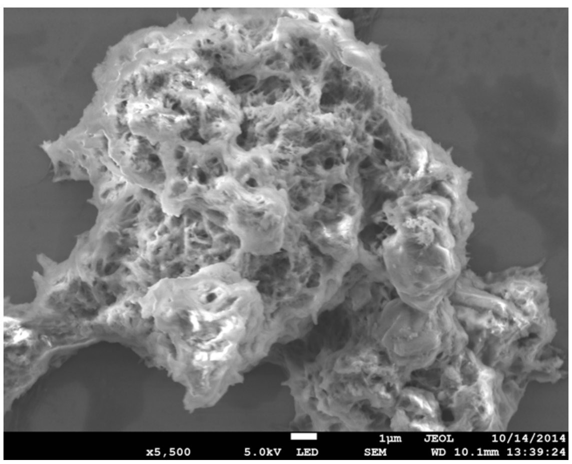
1μm JEOL 10/14/2014
x5,500 5.0kV LED SEM WD 10.1mm 13:39:24

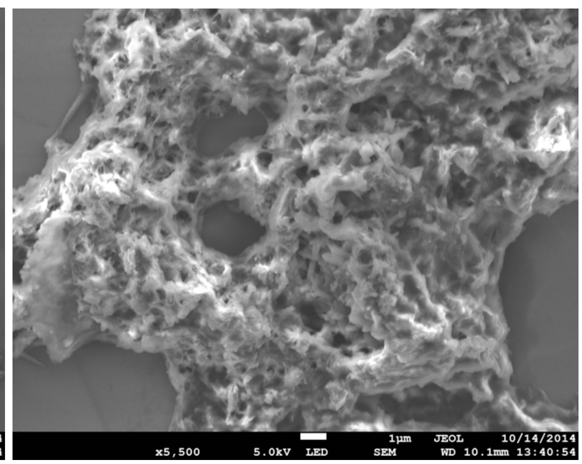
1μm JEOL 10/14/2014
x5,500 5.0kV LED SEM WD 10.1mm 13:40:54

(e) (f)

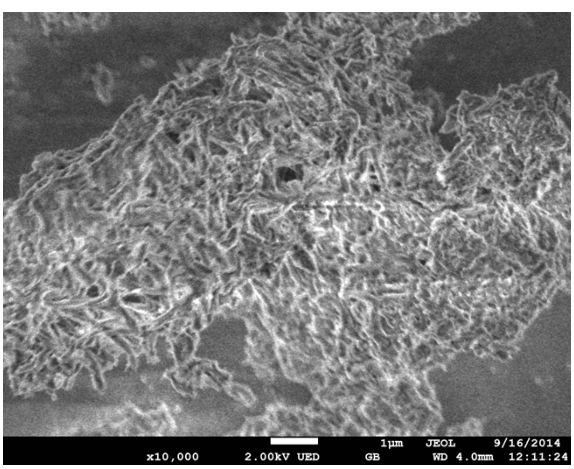
1μm JEOL 9/16/2014
x10,000 2.00kV UED GB WD 4.0mm 12:11:24

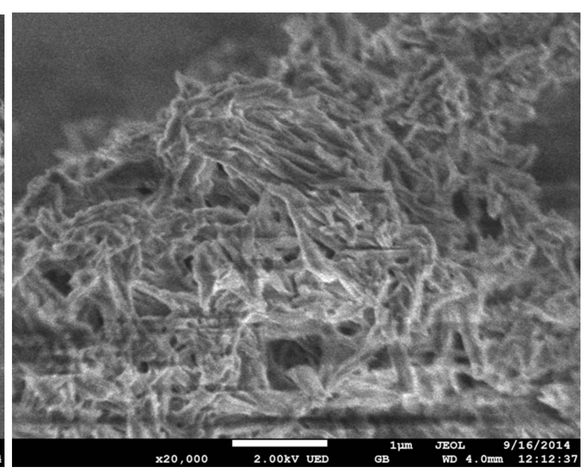
1μm JEOL 9/16/2014
x20,000 2.00kV UED GB WD 4.0mm 12:12:37

(g) (h)

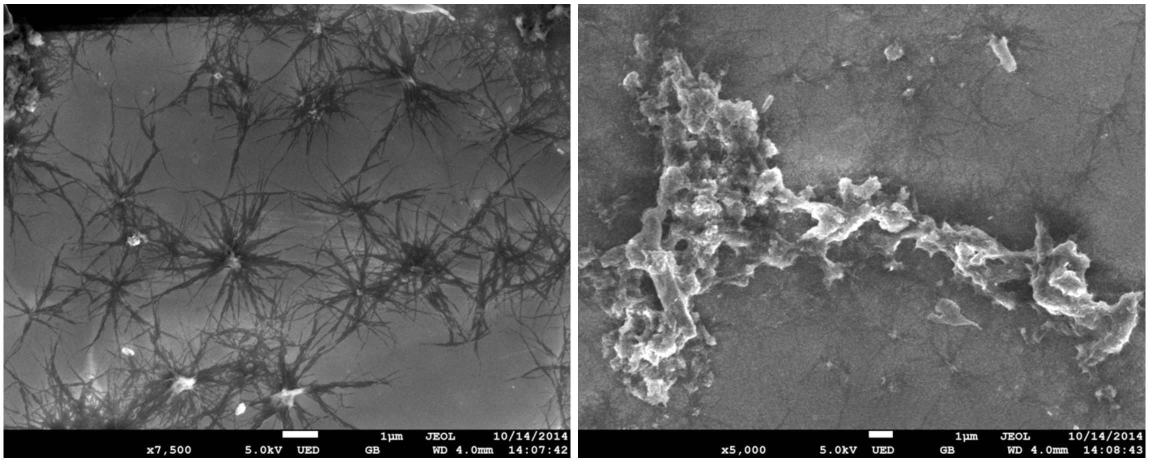

Fig. S2 The SEM images of the separator membrane of MOF **1** before (**a, b**) and after the charge-discharge experiments (**c, d**). The SEM images of the separator membrane of MOF **2** before (**e, f**) and after the charge-discharge experiments (**g, h**).

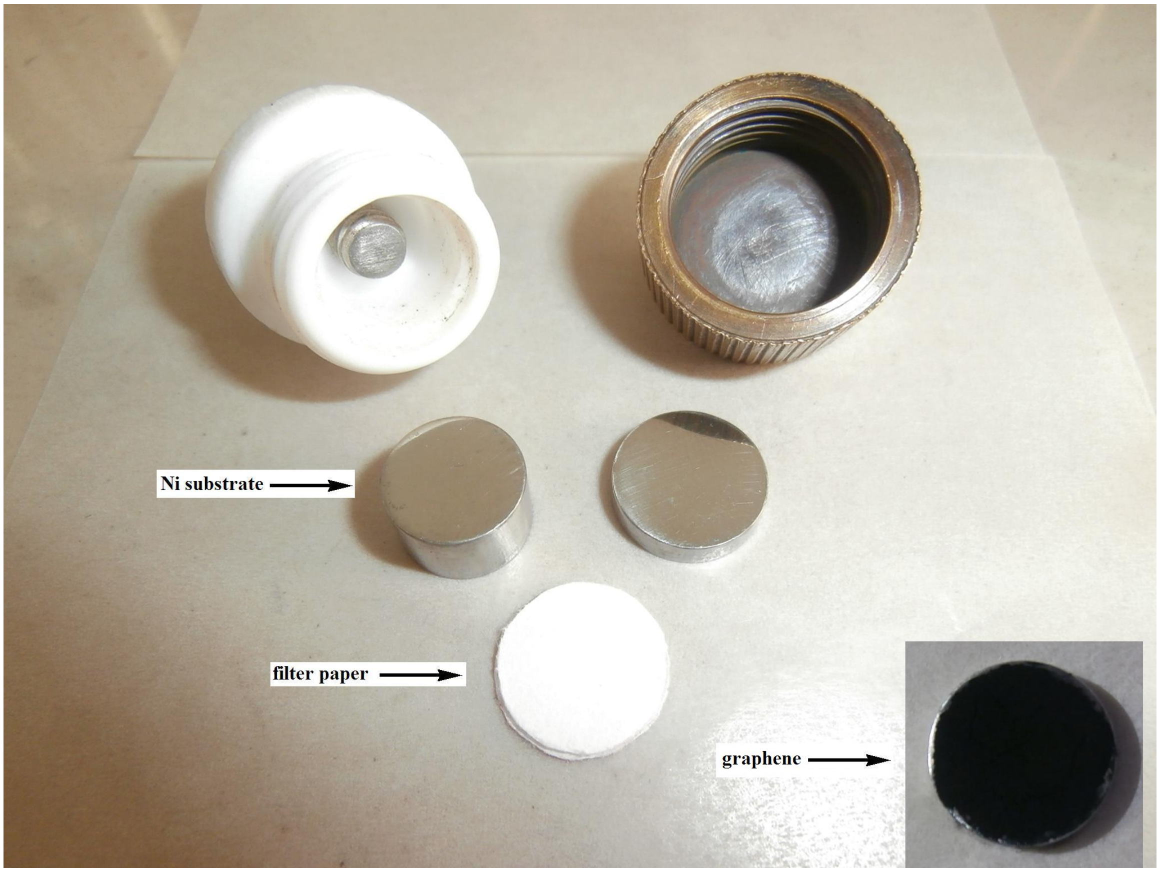

Fig. S3 The images of the supercapacitor, in which two Ni substrates were used as current collectors, and each piece of the collector was covered by 0.25 mg graphene as electrode material. The separator membrane of MOF was sandwiched by two pieces of filter papers with two drops of the $NaNO_3$ aqueous solution on each side as the electrolyte.

(a)

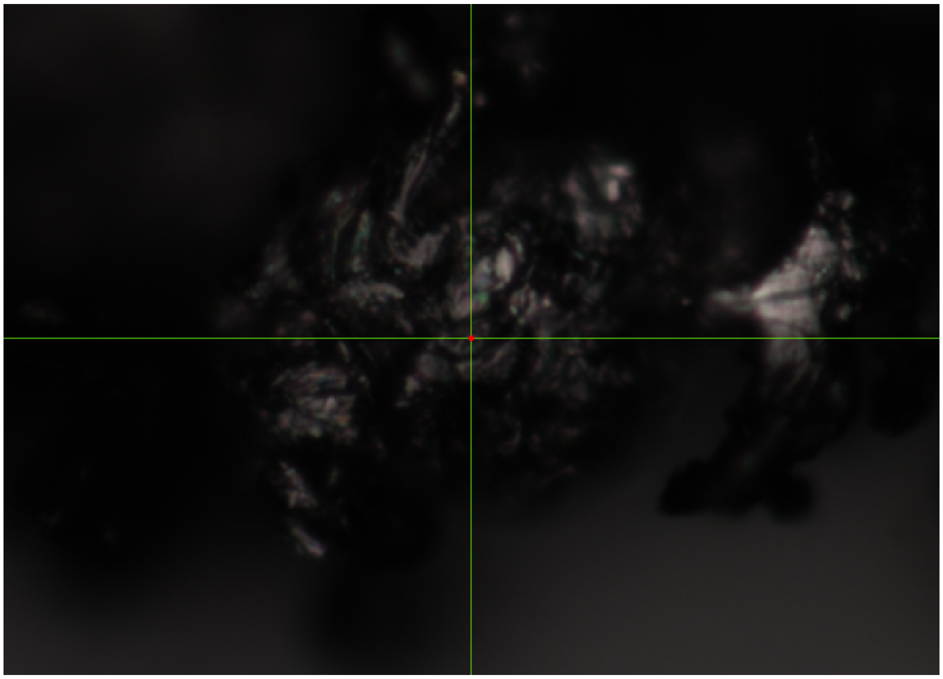

(b)

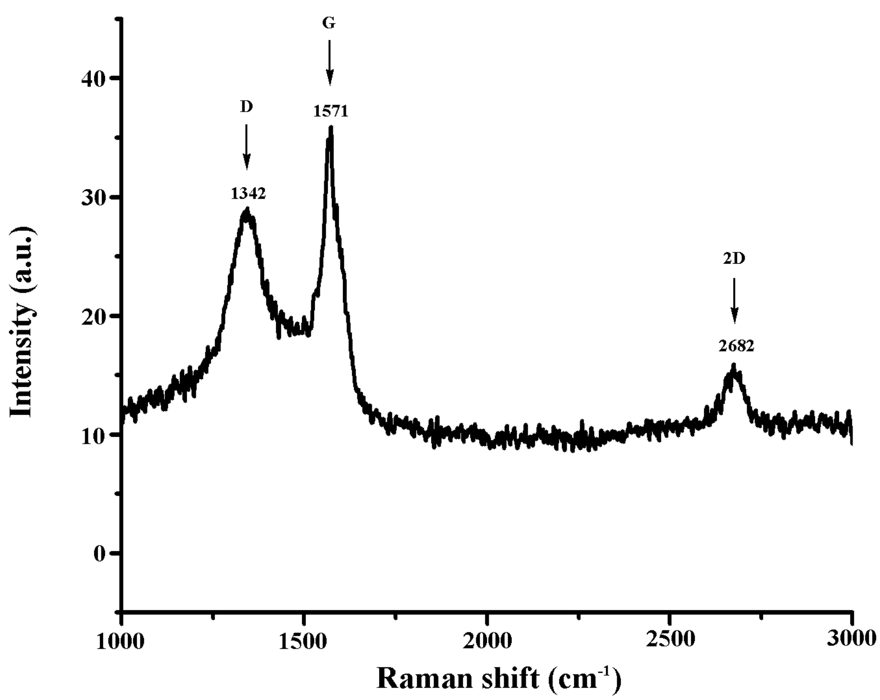

Fig. S4 The image (**a**) and the Raman spectra (**b**) (λ_{ex} = 514.5 nm, 0.4 mW) of the graphene in supercapacitor.

Thermal stability of MOF 3 The TGA curve of MOF **3** show a one step weight loss between 30 and 240 °C corresponding to the loss of the uncoordinated solvent molecules (obsd. 17.9 %, calc. 18.0 wt%). The desolvated MOF **3** remained stable up to 320 °C without any weight loss (**Fig. S5**). Similar desolvation method is applied for MOF **3,** and the desolvated sample possesses its original host framework, as evidenced by the powder XRD patterns (**Fig. S6c**), indicating MOF **3** also possess good thermal stability.

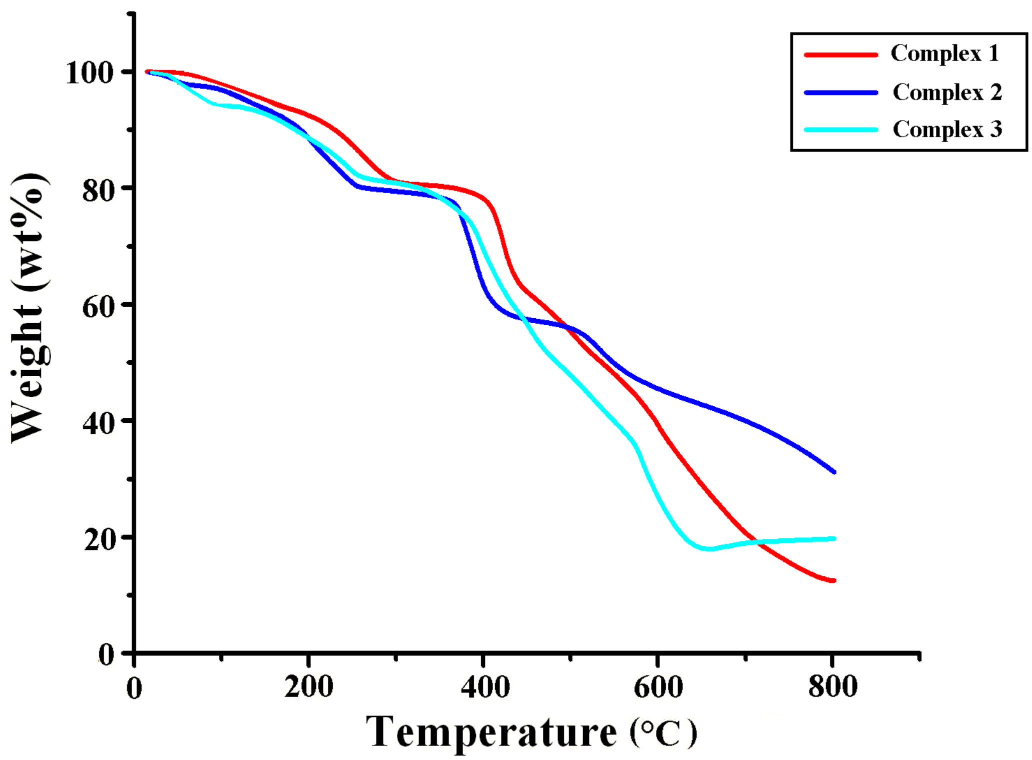

Fig. S5 TG curves of MOFs **1** (red), **2** (blue) and **3** (sapphire).

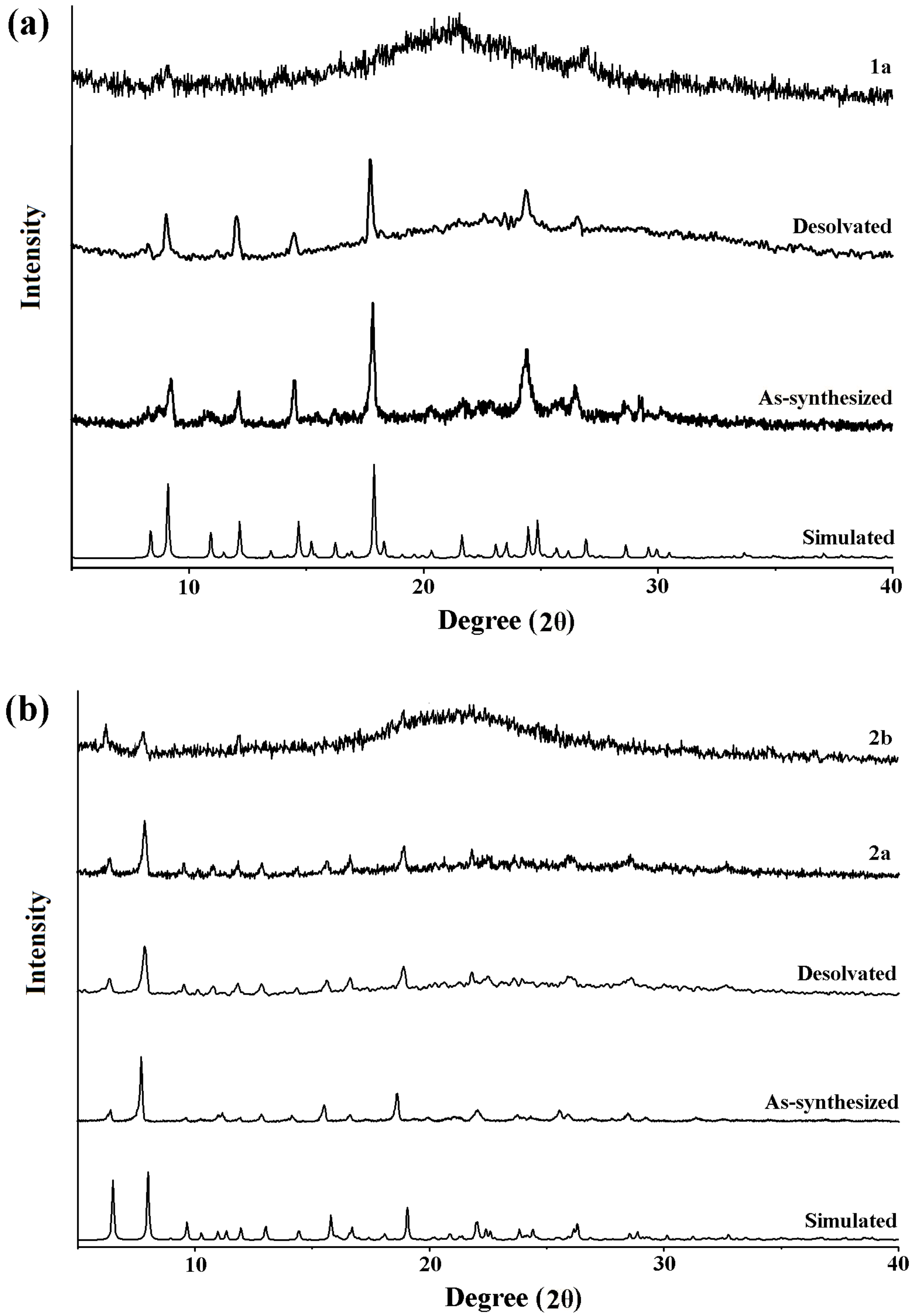
(a)
1a
Desolvated
As-synthesized
Simulated
Intensity
10
20
30
40
Degree (2θ)
(b)
2b
2a
Desolvated
As-synthesized
Simulated
Intensity
10
20
30
40
Degree (2θ)

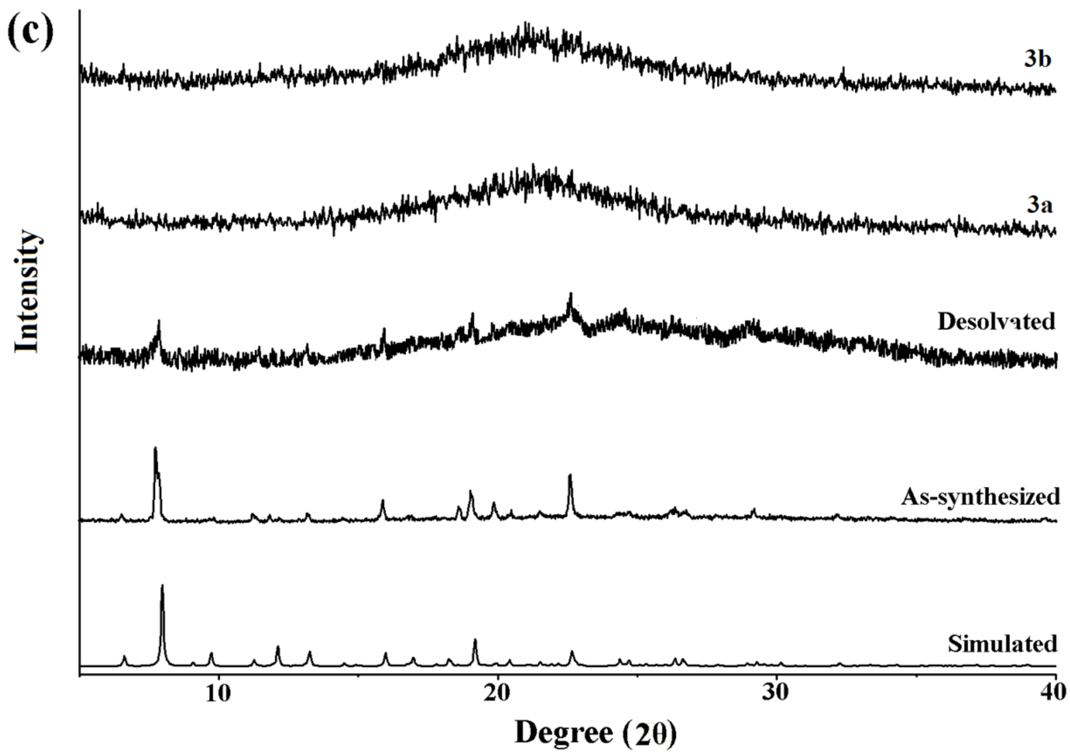

Fig. S6 The PXRD patterns of MOFs **1** (**a**), **2** (**b**) and **3** (**c**).

(a)

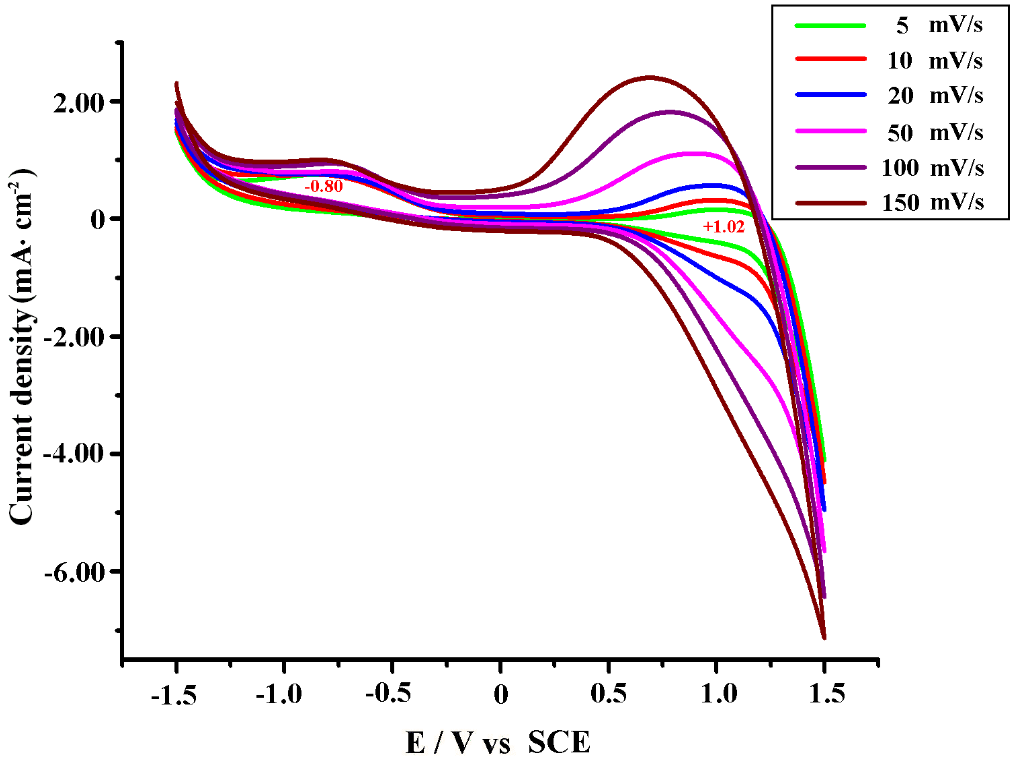
5 mV/s
10 mV/s
20 mV/s
50 mV/s
100 mV/s
150 mV/s
2.00
0
-2.00
-4.00
-6.00
Current density (mA· cm^{-2})
-0.80
+1.02
-1.5
-1.0
-0.5
0
0.5
1.0
1.5
E / V vs SCE

(b)

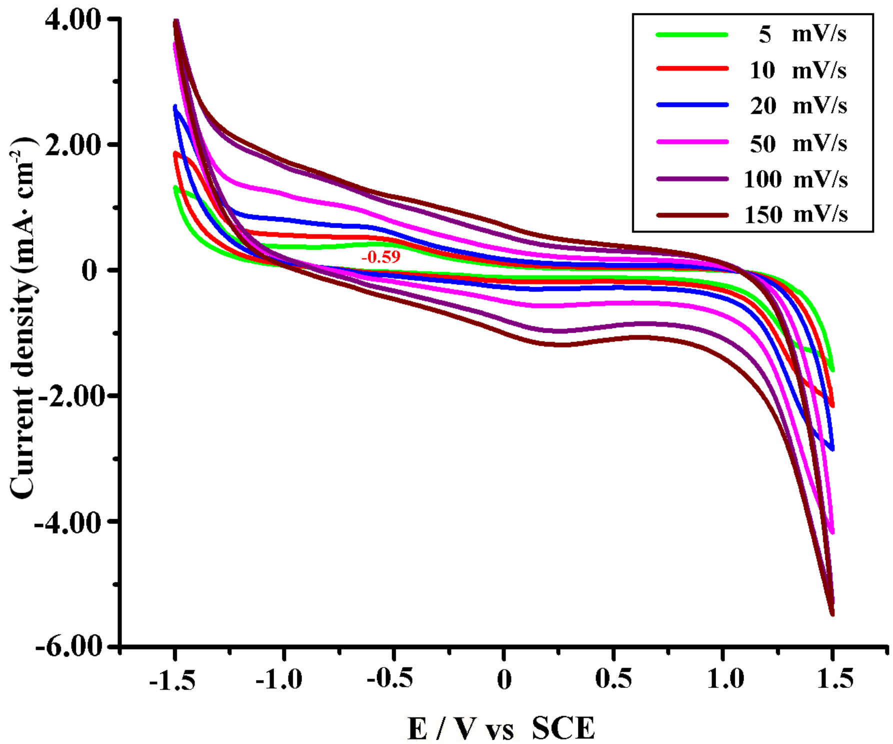
4.00
2.00
0
-2.00
-4.00
-6.00
Current density (mA· cm^{-2})
5 mV/s
10 mV/s
20 mV/s
50 mV/s
100 mV/s
150 mV/s
-0.59
-1.5
-1.0
-0.5
0
0.5
1.0
1.5
E / V vs SCE

(c)

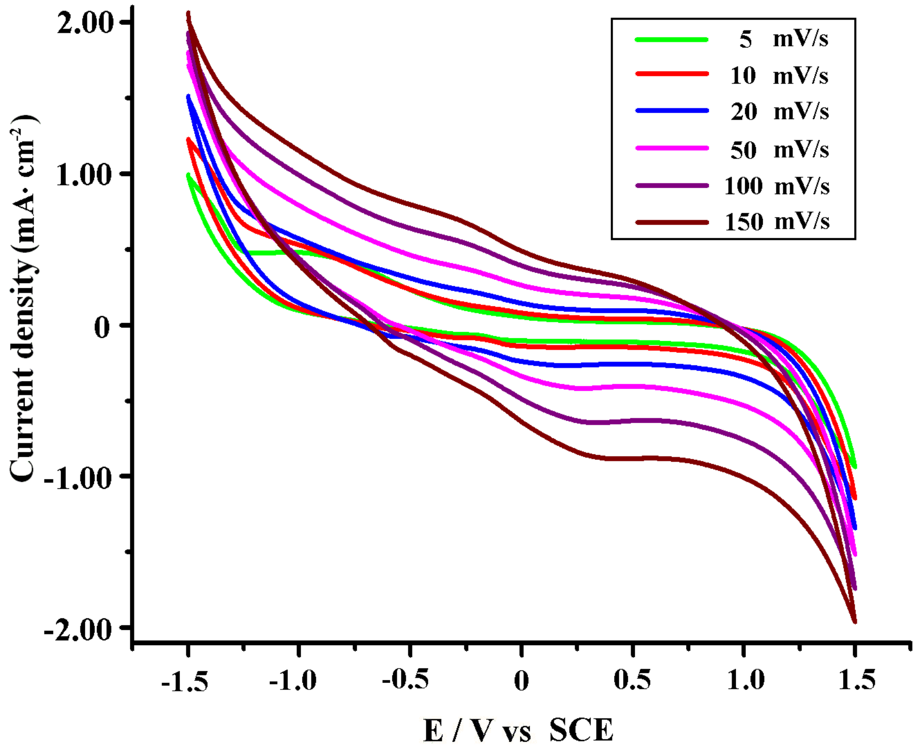

2.00
1.00
0
-1.00
-2.00
Current density (mA· cm-2)
-1.5
-1.0
-0.5
0
0.5
1.0
1.5
E / V vs SCE
5 mV/s
10 mV/s
20 mV/s
50 mV/s
100 mV/s
150 mV/s

(d)

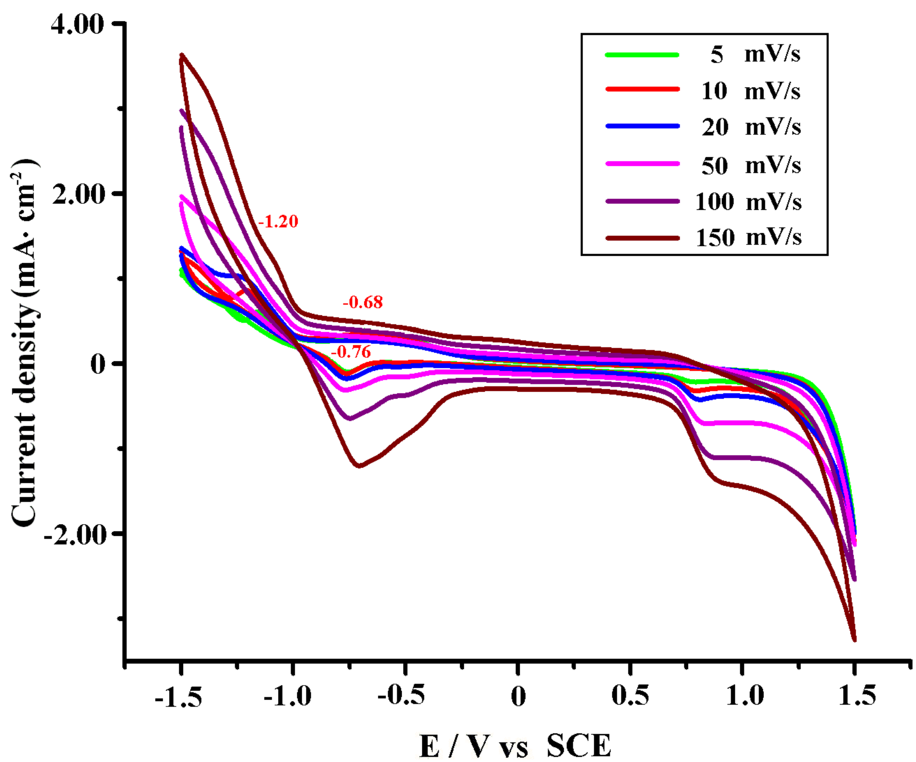

4.00
2.00
0
-2.00
Current density (mA· cm-2)
-1.5
-1.0
-0.5
0
0.5
1.0
1.5
E / V vs SCE
-1.20
-0.68
-0.76
5 mV/s
10 mV/s
20 mV/s
50 mV/s
100 mV/s
150 mV/s

Fig. S7 Cyclic voltammograms of **1-GCE** (**a**), **L-GCE** (**b**), **1,4-H_2bdc-GCE** (**c**) and **2-GCE** (**d**) in a 0.05 M $NaNO_3$ aqueous solution (50 mL) at different sweep rates.

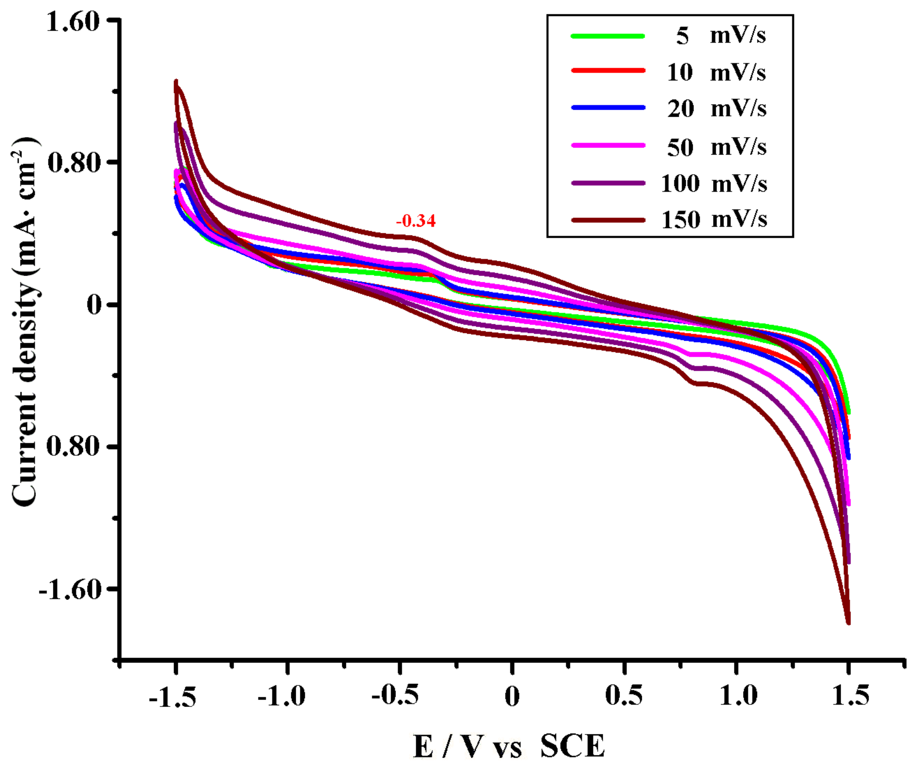

Fig. S8 Cyclic voltammograms of the bare **GCE** in a 0.05 M $NaNO_3$ aqueous solution (50 mL) at different sweep rates.

(a)

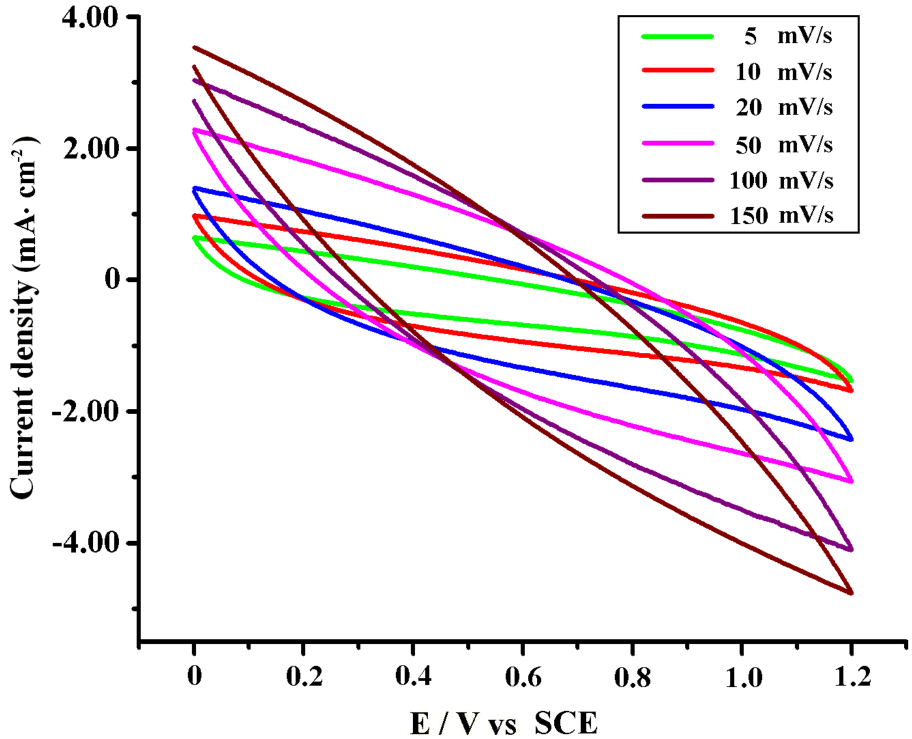

4.00
2.00
0
-2.00
-4.00
Current density (mA· cm^{-2})
0
0.2
0.4
0.6
0.8
1.0
1.2
E / V vs SCE
5 mV/s
10 mV/s
20 mV/s
50 mV/s
100 mV/s
150 mV/s

(b)

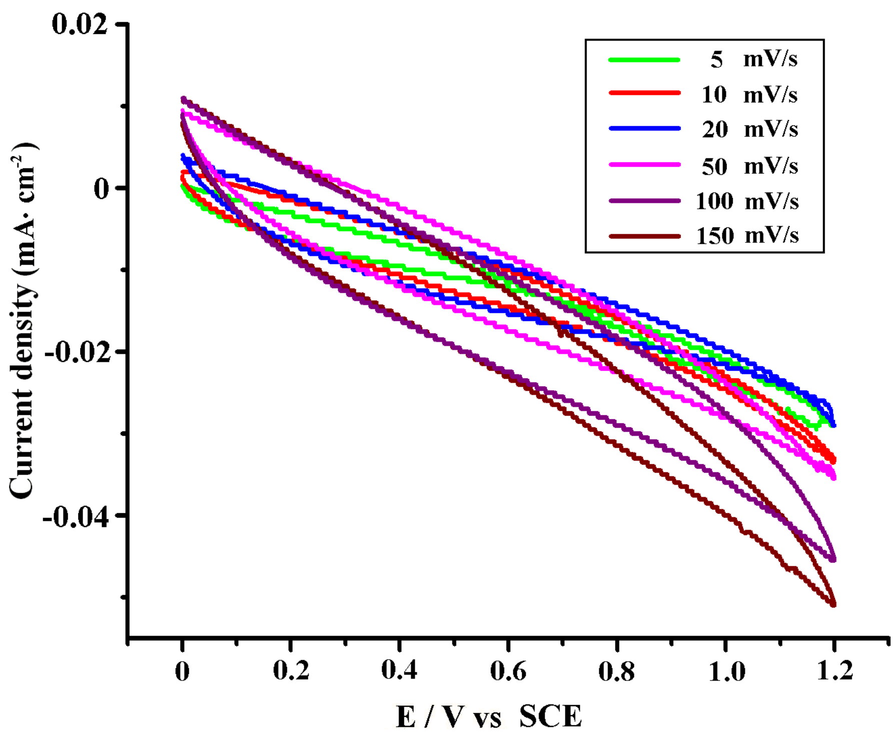

0.02
0
-0.02
-0.04
Current density (mA· cm^{-2})
0
0.2
0.4
0.6
0.8
1.0
1.2
E / V vs SCE
5 mV/s
10 mV/s
20 mV/s
50 mV/s
100 mV/s
150 mV/s

(c)

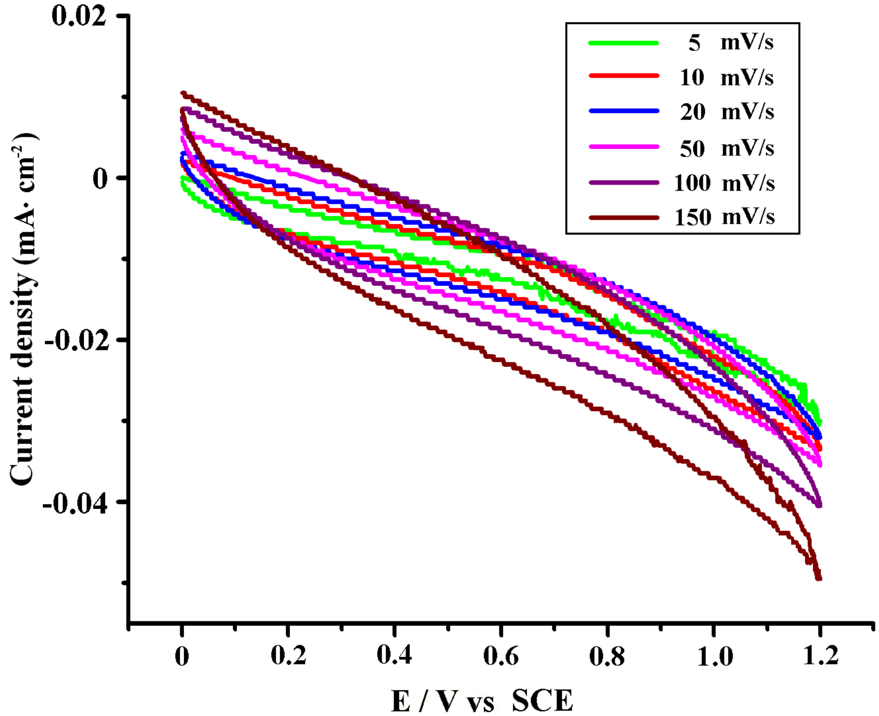

Fig. S9 CVs of the supercapacitor in the absence (**a**) and presence of the separator membranes of MOFs **1** (**b**) and **2** (**c**) at different sweep rates. Supporting electrolyte = 0.05 M $NaNO_3$ aqueous solution.

(a)

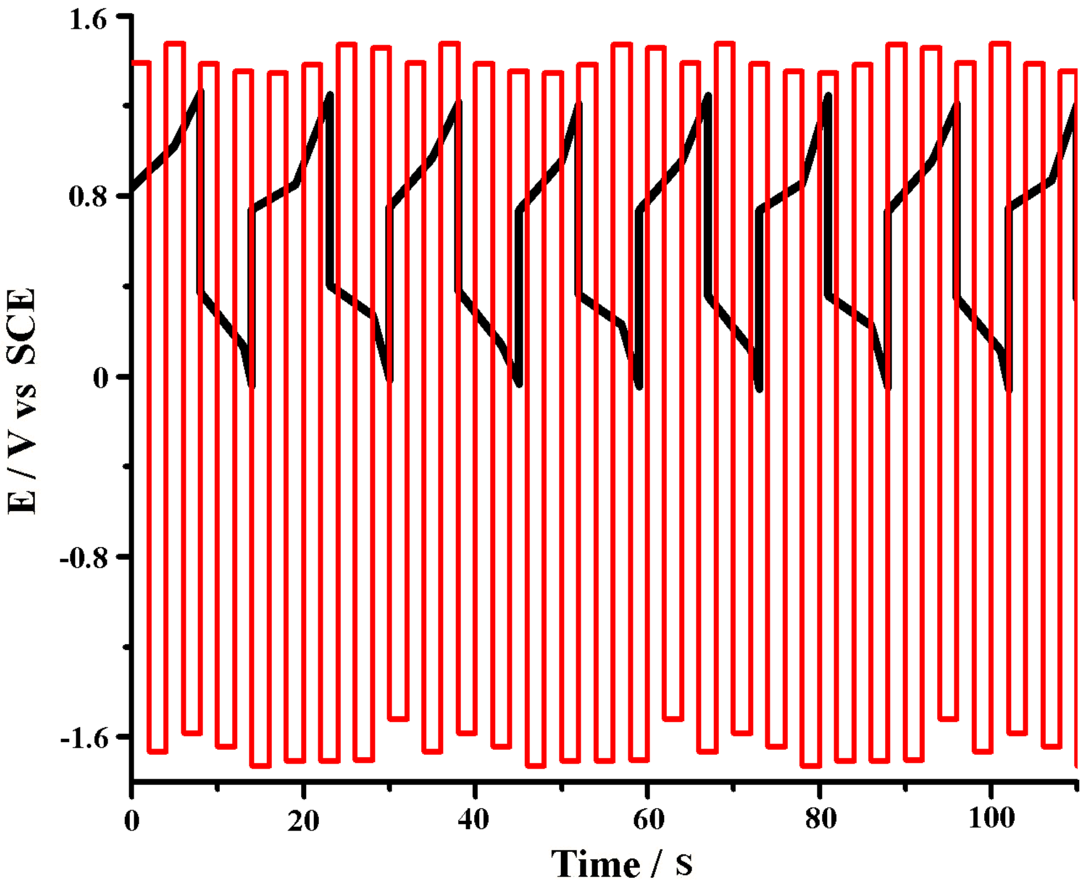

(b)

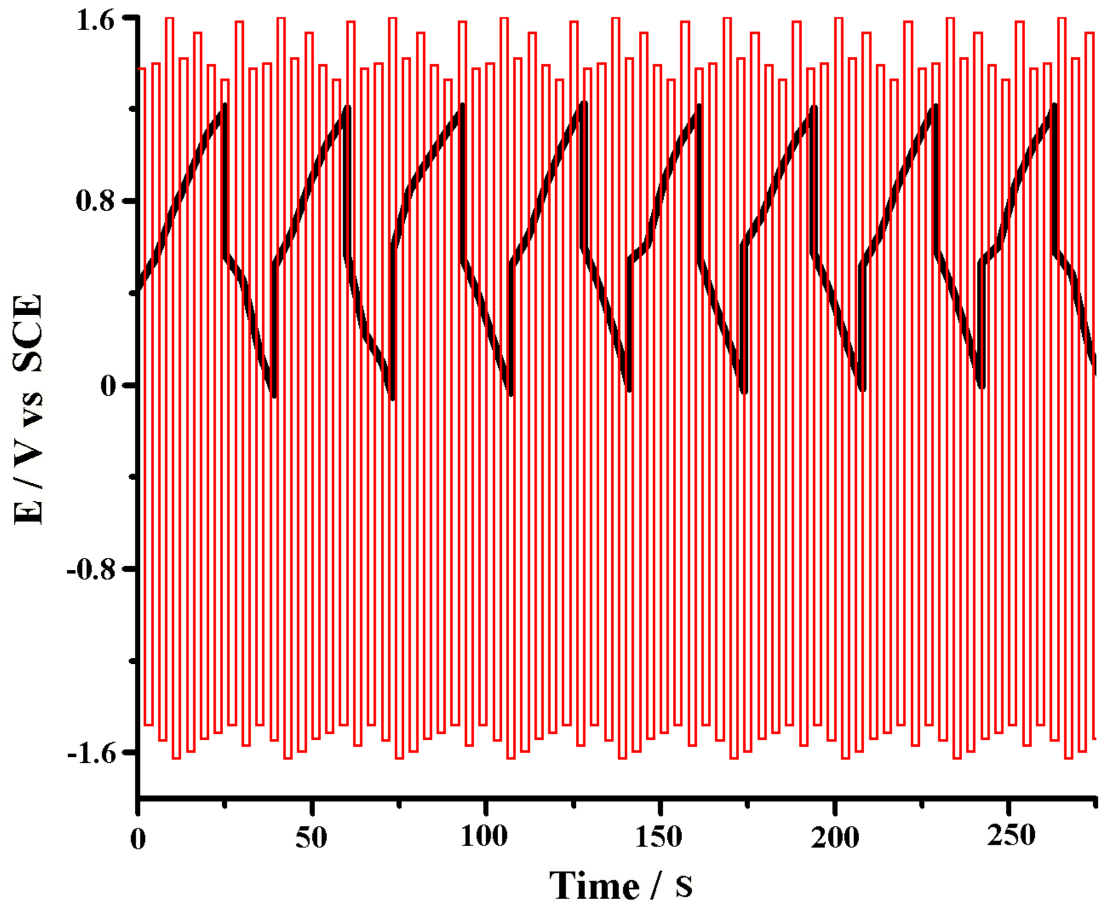

Fig. S10 Typical charge-discharge cycles obtained in the presence (red) and absence (black) (**c**) of the separator membrane of MOF **1** at 3.0 A·g^{-1} (**a**) and 2.0 A·g^{-1} (**b**), respectively. Supporting electrolyte = 0.05 M $NaNO_3$ aqueous solution.

The specific capacitance (SC) based on the graphene was estimated from the discharge process using **Equations 1** as follow: [1]

$$SC\ (F\cdot g^{-1}) = (I \times \Delta t)/(\Delta E \times m) \quad (\mathbf{1})$$

where I, $\triangle t$, $\triangle E$ and m represent the current density, discharge time, potential range and the mass of the graphene, respectively.

As shown in the **Scheme S1**, the equivalent series resistance (R_{es}) was obtained from **Equation 2**. [2]

$$R_{es}\ (Ohm) = \Delta V / (2i) \quad (\mathbf{2})$$

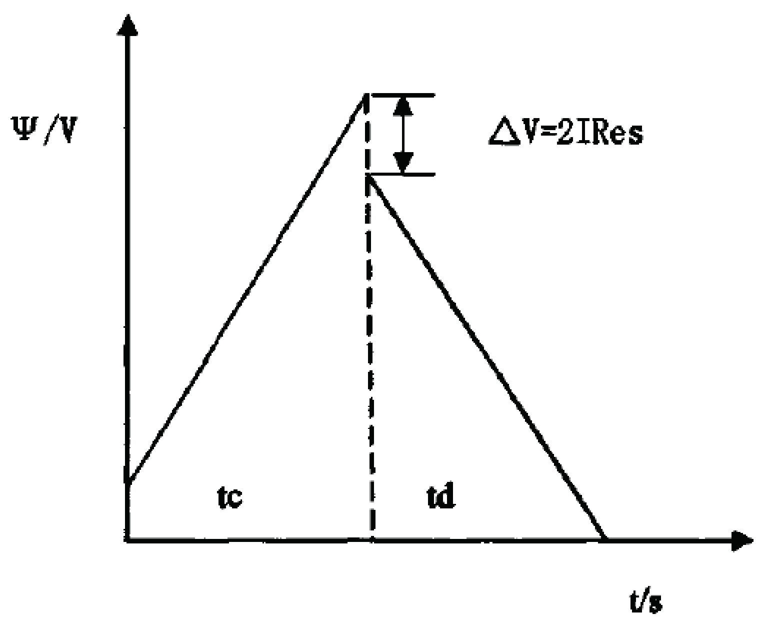

Scheme S1 Potential profiles of charge / discharge of supercapacitor at constant current

The energy deliverable efficiency (η/%) was obtained from **Equation 3.** [3]

$$\eta\ (\%) = t_d / t_c \times 100 \quad (\mathbf{3})$$

where t_d and t_c are discharge time and charging time, respectively.

Table S2 Supercapacitive properties in the absence and presence of the separator membrane of MOF **1** or **2** determined using the galvanostatic discharge method at different current densities (Supporting electrolyte = 0.05 M $NaNO_3$ aqueous solution; Potential range = 0～1.2 V).

Current Density/ $A \cdot g^{-1}$	**Separator membrane**	**Supercapacitive parameters**			
		Discharge Time/ s	**R_{es} / Ohm**	**SC/ $F \cdot g^{-1}$**	**η/ %**
3.0	Without MOF-based separator membrane	6	533	15	75
2.0	Without MOF-based separator membrane	10	630	16.7	62
0.3	Without MOF-based separator membrane	84	733	21	88.4
	With MOF **1**-based separator membrane	260	1133	65	96
	With MOF **2**-based separator membrane	8	5333	2	80
0.2	Without MOF-based separator membrane	139	1000	23.2	82.7
	With MOF **1**-based separator membrane	400	2000	66.7	90
	With MOF **2**-based separator membrane	16	6500	2.7	57.1

(a)

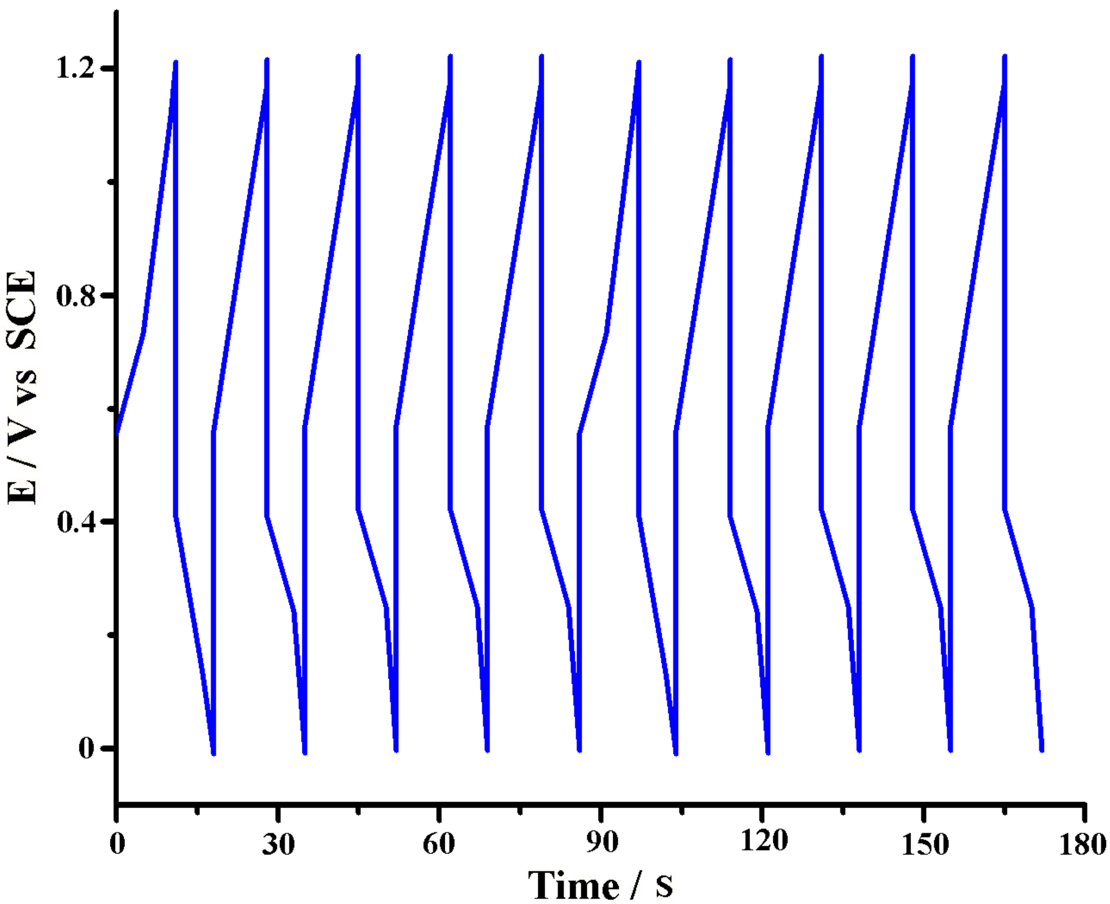

(b)

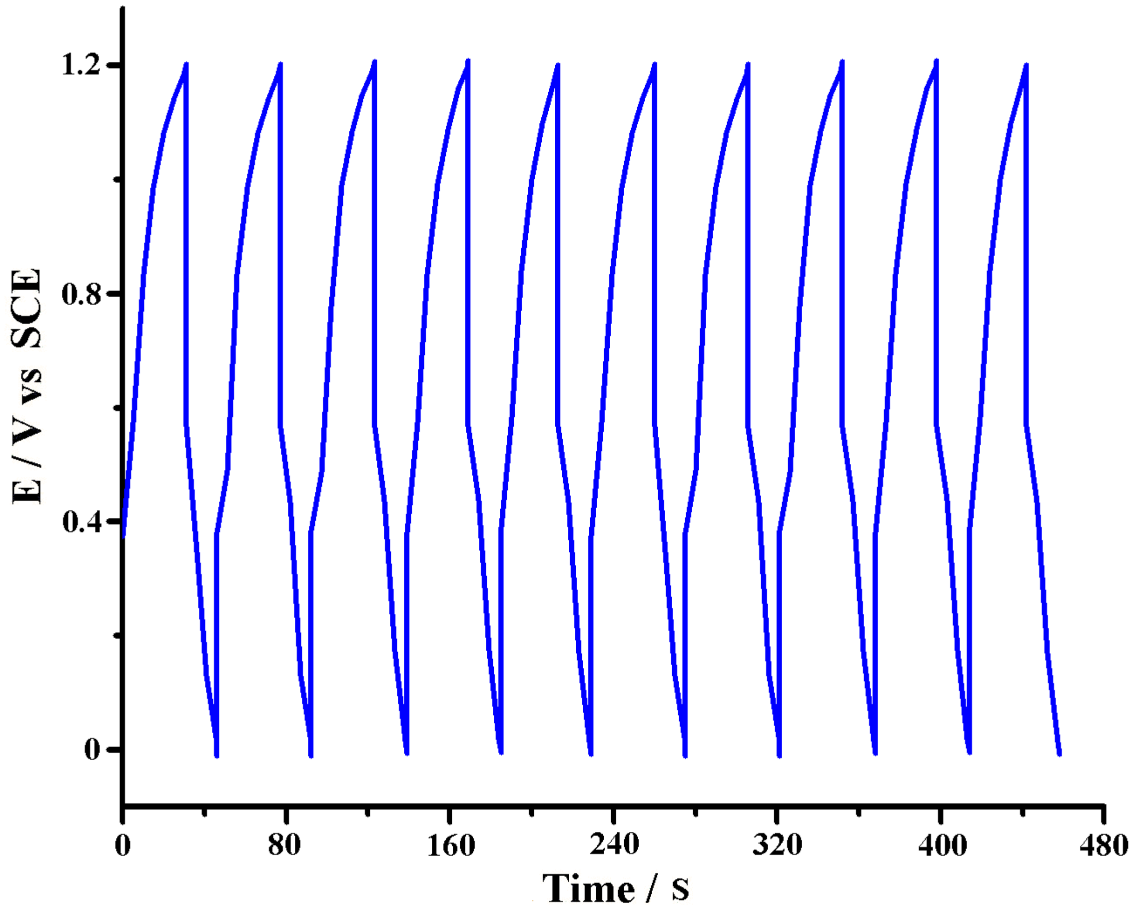

Fig. S11 Typical charge-discharge cycles obtained in the presence of the separator membrane of MOF **2** at 0.3 $A \cdot g^{-1}$ (**a**) and 0.2 $A \cdot g^{-1}$ (**b**), respectively. Supporting electrolyte = 0.05 M $NaNO_3$ aqueous solution.

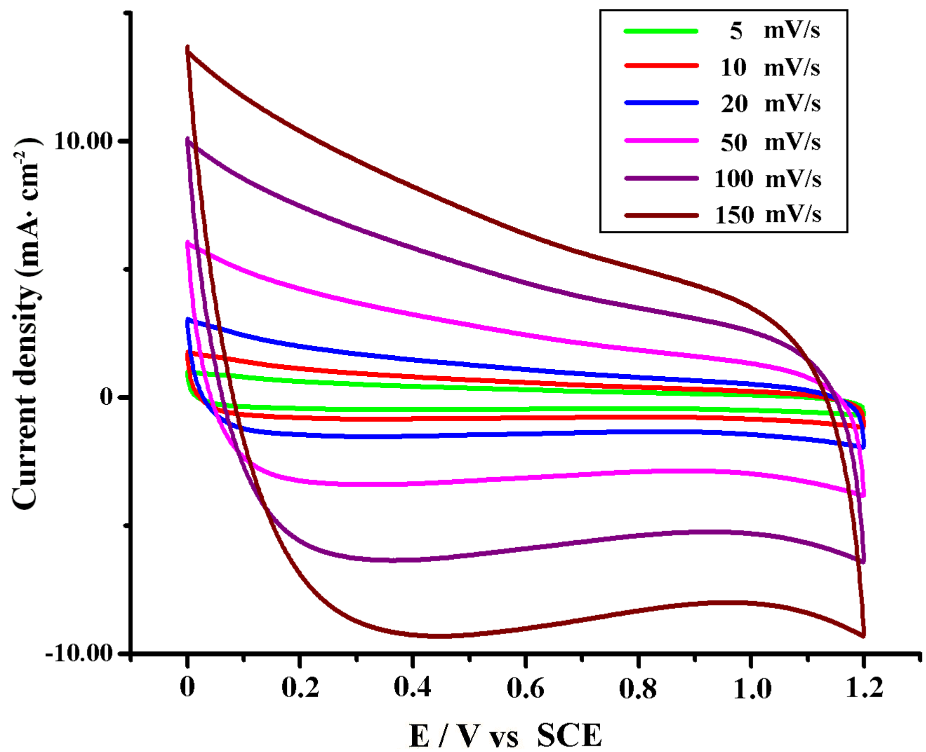

Fig. S12 CVs of the supercapacitor in the presence of the separator membrane of **1a** at different sweep rates. Supporting electrolyte = 0.05 M $NaNO_3$ aqueous solution.

(**a**)

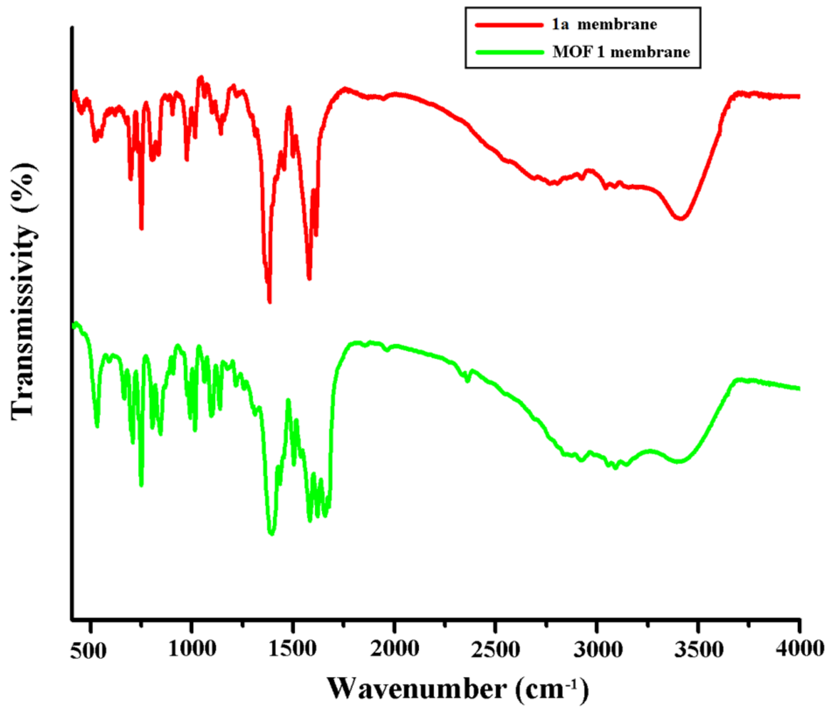

(**b**)

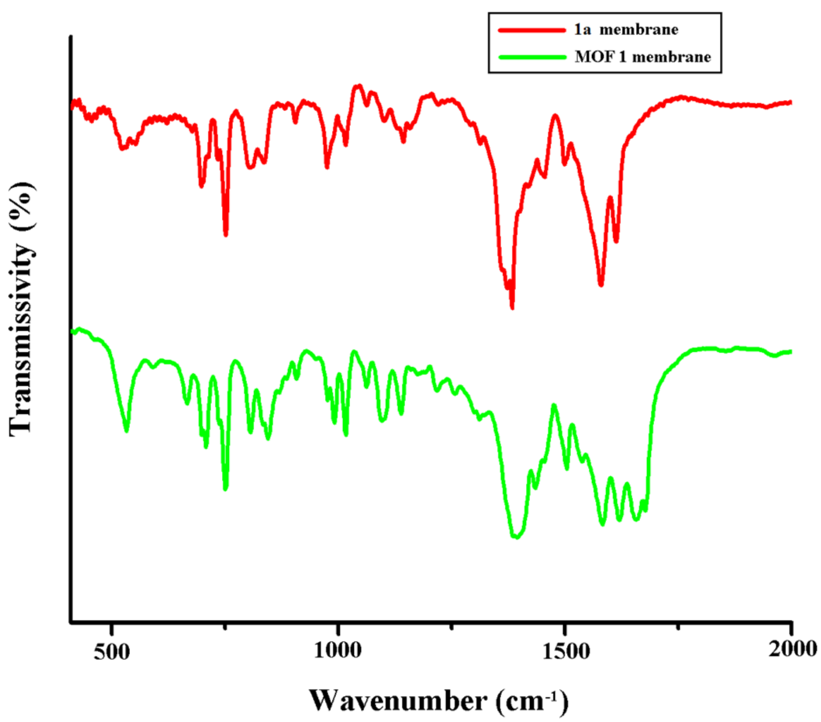

Fig. S13 The IR spectra of the separator membranes of **1a** and **1** in different scales (**a**, **b**).

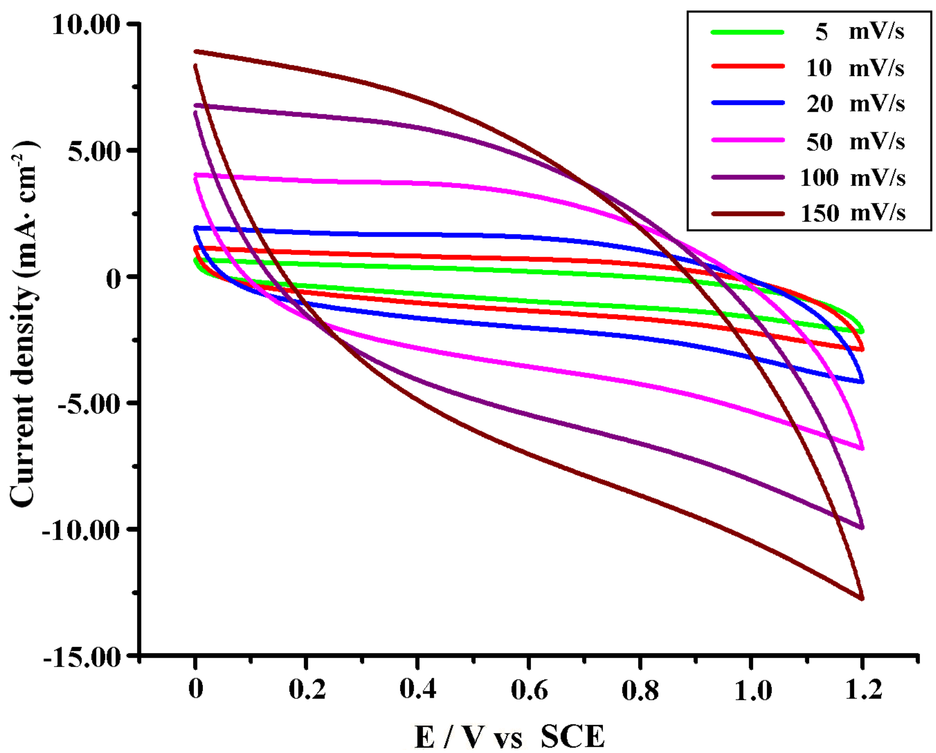

Fig. S14 CVs of the supercapacitor in the presence of the separator membrane of **1a** at different sweep rates. Supporting electrolyte = 0.05 M phosphate buffer aqueous solution (pH 6.8, H_3PO_4/NaOH).

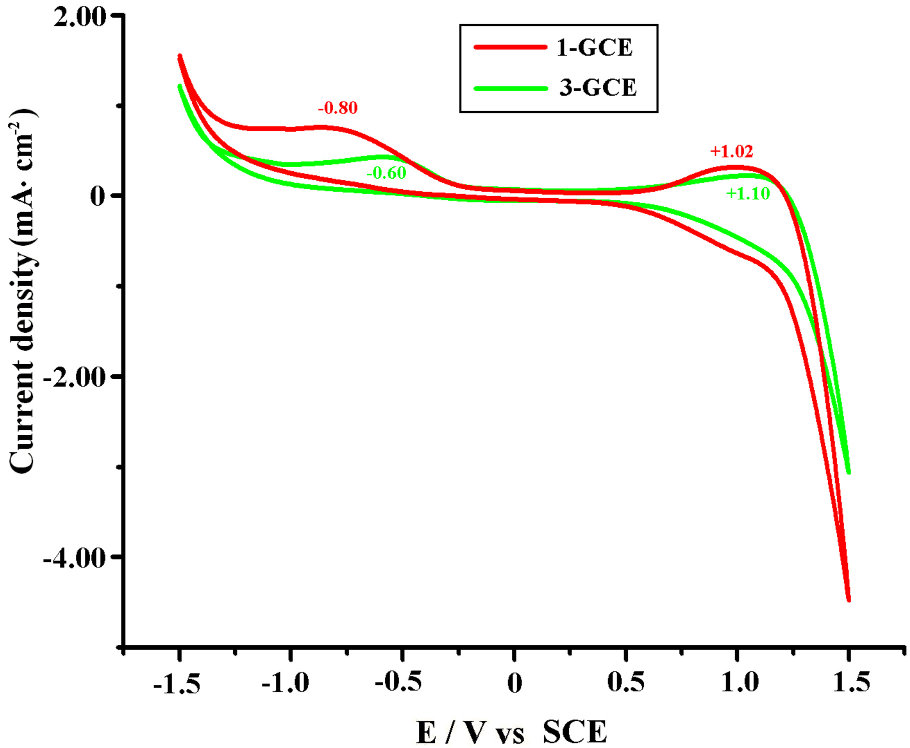

Fig. S15 CVs of **1-GCE** (red) and **3-GCE** (green) in a 0.05 M $NaNO_3$ aqueous solution (50 mL) at a scan rate of 10 $mV{\cdot}s^{-1}$.

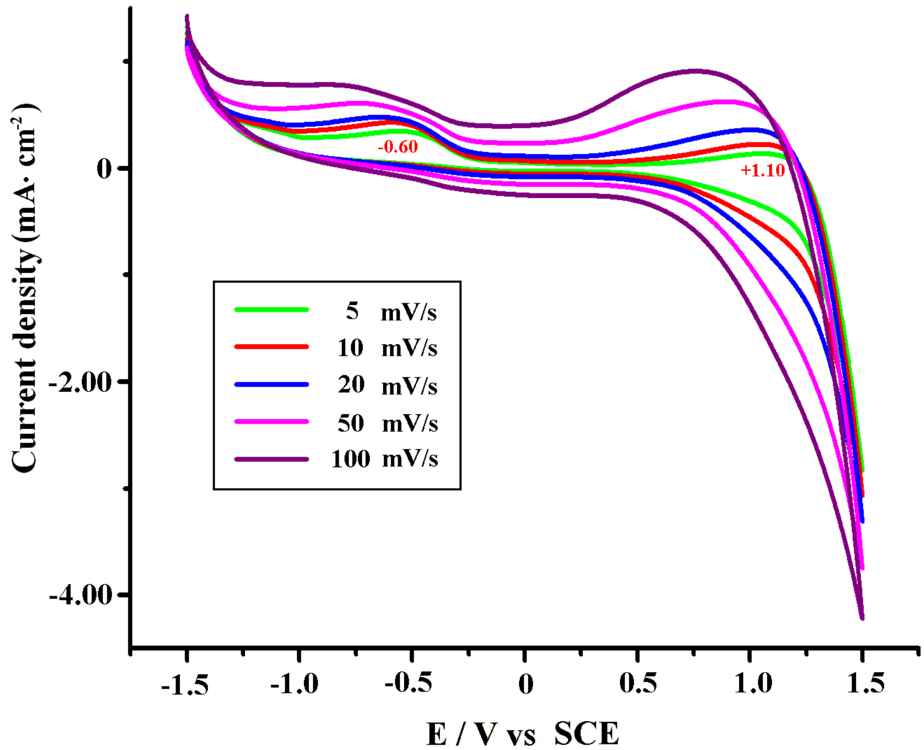

Fig. S16 Cyclic voltammograms of **3-GCE** in a 0.05 M $NaNO_3$ aqueous solution (50 mL) at different sweep rates.

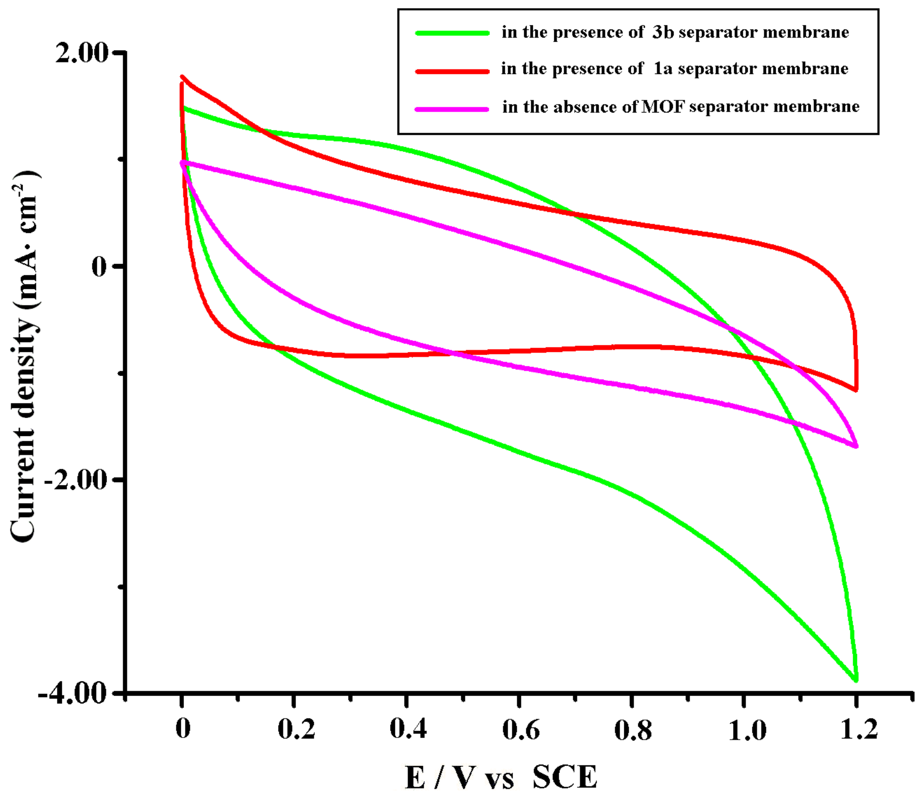

Fig. S17 CVs of the supercapacitors in the absence and presence of the separator membrane of **1a** and **3b** at a scan rate of 10 $mV \cdot s^{-1}$. Supporting electrolyte = 0.05 M $NaNO_3$ aqueous solution.

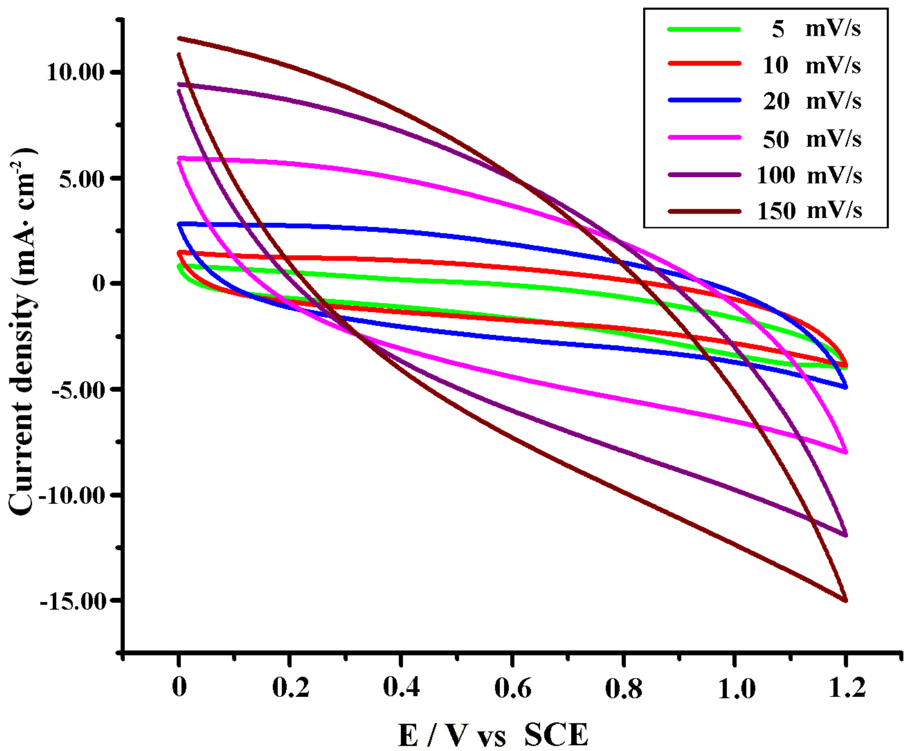

Fig. S18 CVs of the supercapacitor in the presence of the separator membrane of **3b** at different sweep rates. Supporting electrolyte = 0.05 M $NaNO_3$ aqueous solution.

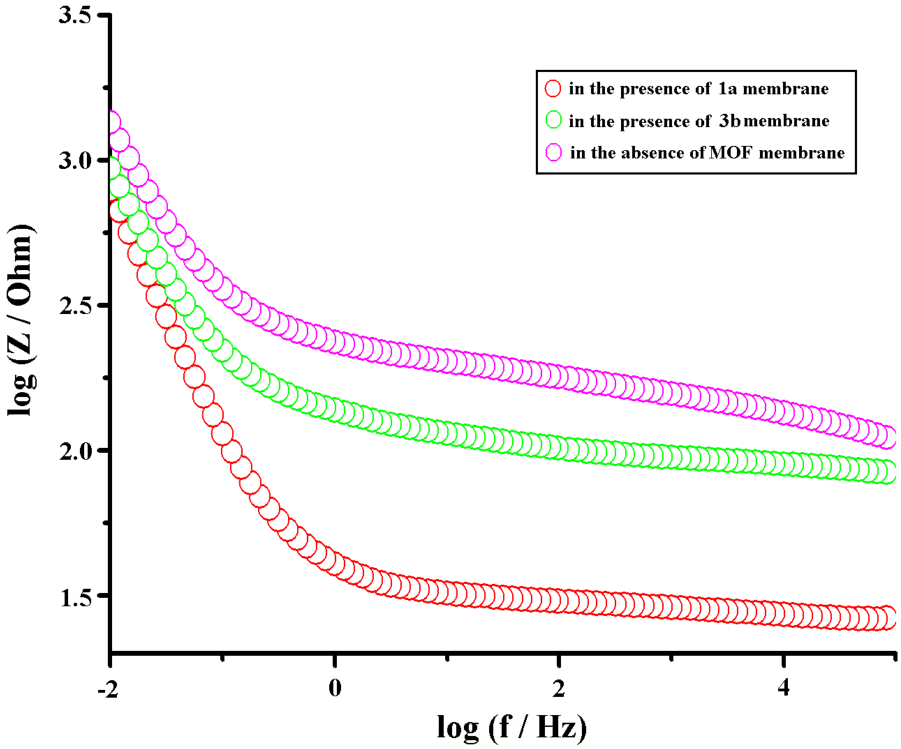

Fig. S19 Bode plots (log of impedance magnitude vs. log f) the supercapacitors at the initial potential of 0 V in the absence and presence of the separator membrane of MOF **1a** and **3b**. Supporting electrolyte = 0.05 M $NaNO_3$ aqueous solution.

References:

1 (a) K. R. Prasad and N. Munichandraiah, *Electrochem. Solid-State Lett.*, **2002**, *5*, A271; (b) V. Gupta, T. Shinomiya, N. Miurain: *Recent Advances in Supercapacitors*, ed. V. Gupta, Transworld Research Network, Kerala, India, **2006**, (ch. 2), 17; (c) V. Ganesh, S. Pitchumani and V. Lakshminarayanan, *J. Power Sources*, **2006**, *158*, 1523; (d) T. Shinomiya, V. Gupta and N. Miura, *Electrochim. Acta*, **2006**, *51*, 4412.

2 W. G. Pell and B. E. Conway, *J. Electroanal. Chem.*, **2001**, *500*, 121.

3 S. G. Kandalkar, J. l. Gunjakar and C. D. Lokhande, *Appl. Surf. Sci.*, **2008**, *254*, 5540.